$Y_l^m(\theta,\phi)$ are the usual spherical harmonics and $(am, bm'|cM)$ is a Clebsch-Gordan coefficient. Tables by Rose are useful in computing these Θ functions.[25]

Note that some terms in the above correlation are symmetrical about the beam direction and others are symmetrical about the direction of the inelastically scattered particle. Only $L \leq 2$ and $L' \leq 2$ are considered. Table I shows that this probably includes $\sim 85\%$ of the reaction. Higher L values were not considered because of the complexity of the calculation.

[25] M. E. Rose, Oak Ridge National Laboratory Report ORNL-2516, 1958 (unpublished).

PHYSICAL REVIEW VOLUME 114, NUMBER 2 APRIL 15, 1959

Elastic Scattering of 40-Mev Protons from Isotopes of Fe, Ni, and Cu†

MORTON K. BRUSSEL* AND JOHN H. WILLIAMS‡
University of Minnesota, Minneapolis, Minnesota

(Received November 26, 1958)

39.8-Mev protons were scattered from thin targets of Fe^{54}, Fe^{56}, Ni^{58}, Ni^{60}, and Cu^{65}. Absolute differential cross sections obtained with a statistical accuracy of $\leqq 3\%$ have been determined for the elastically scattered protons. The range of the angular distributions, 7.5° to 110°, encompassed three minima and three maxima in the measured cross sections. The energy resolution of the detection equipment, utilizing a NaI(Tl) crystal, was 1.2-2%. This enabled a separation to be made of elastic from nonelastic events. A detector telescope allowed angular resolutions of $\pm\frac{1}{8}°$ to be used in determining the shape of the features in the angular distributions. The general variation of the cross sections with the nuclear mass is noted. In addition, the data suggest that the nucleon shell closing about nucleon number 28 introduces fine structure differences in the shape and magnitude of features of the scattering pattern.

I. INTRODUCTION

MEASUREMENTS of angular distributions of protons elastically scattered from various elements provide one of the most amenable methods of determining nuclear force properties, since they give information about the shape and strength of the effective scattering potential active between proton and nucleus.

Burkig and Wright,[1] at 18.6 Mev, were the first to investigate nuclear effects of proton scattering in heavier elements. Although they missed the details present in the angular distributions, they did note that as the atomic number of their targets increased, the ratio of total elastic scattering differential cross sections to Rutherford scattering cross sections decreased.

Baker, Dodds, and Simmons[2] noticed at 10 Mev that specific features in the angular distribution of the elastically scattered protons tended to move towards smaller angles as the atomic number of the target nuclei increased. However, the first comprehensive study of proton elastic scattering differential cross sections was performed by Cohen and Neidigh[3] with 22-Mev protons. Plotting ratios of scattering differential cross sections to Rutherford scattering differential cross sections, they found systematic behavior of the features in the angular distributions as a function of atomic number, suggesting optical-like characteristics of nuclear matter.

The interest in elastic proton scattering generated by Cohen and Neidigh resulted in the accumulation of data from many other sources. The first accurate data, where elastically scattered protons were separated and distinguished from nonelastically scattered protons originating in the lowest excited states of the target elements, were compiled by Dayton[4] at 18 Mev. Here, due to greater energy resolution in the data, the scattering features were more pronounced. Only the elastic protons were counted; minima in the former data of Cohen and Neidigh were shallower due to nonelastic scattering contributions.

Subsequently much work has been done with protons in the energy interval 10–40 Mev. References to this work completed before 1957 can be found in the report of Hintz[5] for proton elastic scattering at 10 Mev. Higher energy elastic scattering data has been of more limited accuracy due to the inherently poorer energy resolution available with existing detection systems.

Measurements of proton elastic scattering have been mainly stimulated by the successes of the optical model, wherein a nucleus is represented as a partially absorptive ellipsoid. The most recent and comprehensive applications of this model to proton scattering have been made by Melkanoff,[6] Glassgold,[7] and their co-workers.

† This work was supported in part by the U. S. Atomic Energy Commission.

* Now at Brookhaven National Laboratory, Upton, New York.
‡ Now Director of Division of Research, U. S. Atomic Energy Commission, Washington, D. C.

[1] I. W. Burkig and B. T. Wright, Phys. Rev. **82**, 451 (1951).
[2] Baker, Dodds, and Simmons, Phys. Rev. **85**, 1051 (1952).
[3] B. L. Cohen and R. V. Neidigh, Phys. Rev. **93**, 202 (1954).
[4] I. E. Dayton, Phys. Rev. **95**, 754 (1954).
[5] N. M. Hintz, Phys. Rev. **106**, 1201 (1957).
[6] Melkanoff, Nodvik, Saxon, and Woods, Phys. Rev. **106**, 793 (1957).
[7] Glassgold, Cheston, Stein, Schuldt, and Erickson, Phys. Rev. **106**, 1207, (1957); A. E. Glassgold and P. J. Kellogg, Phys. Rev. **107**, 1372 (1957); Annual Progress Report, 1957–1958, University of Minnesota Linear Accelerator Laboratory, Minneapolis, Minnesota (unpublished).

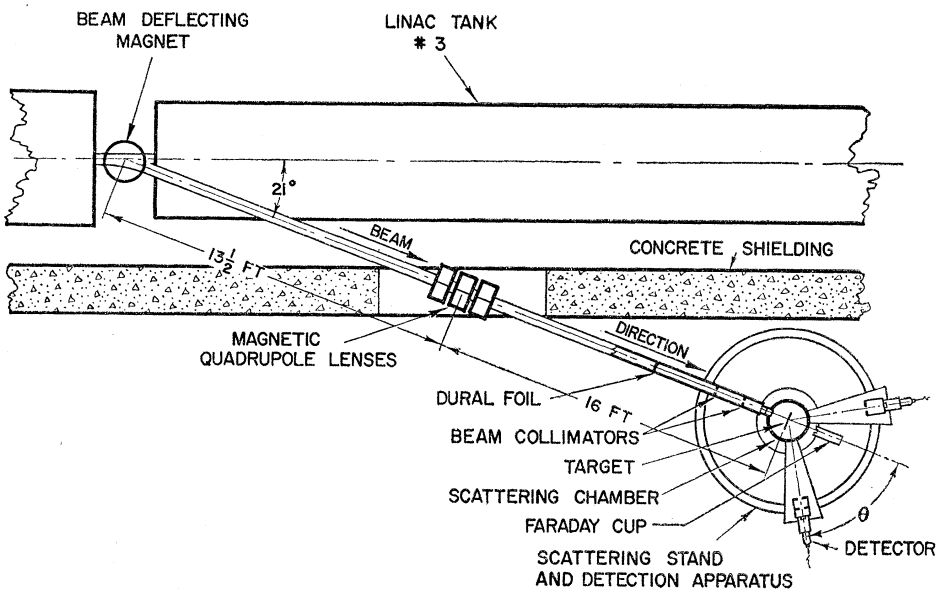

FIG. 1. The experimental arrangement for proton-scattering measurements.

These authors used for the nuclear part of the interaction, spherical potentials of the form[8] $(V_0+iW_0)/\{1+\exp[(r-R)/a]\}$ to fit proton cross-section measurements at 17, 31.5, and 10 Mev. Coulomb potentials of different charge distributions were employed.

As a result of the optical-model analyses of proton elastic scattering, a clearer description of the structure of medium to heavy nuclei has been obtained. Values for the surface diffuseness, a, the absorption, W_0, and the real part of the potential, V_0, have been obtained which are consistent with more fundamental theoretical estimates.

In addition to theoretical ambiguities in determining the parameters from the data as given, the experimental data themselves have not been sufficiently accurate to eliminate ambiguity in their interpretation. Thus, the energy resolution of the detection equipment used in elastic scattering experiments has in general been too poor to distinguish elastically scattered particles from nonelastically scattered ones. Consequently, absolute cross sections measured at backward angles and at minima in the diffraction pattern have been unreliable, for at such angles, nonelastic scattering from energy levels of the target nucleus constitutes a large fraction of the total scattering. Also, the targets used in the scattering experiments have been made of elements with natural isotopic abundances, so that details of the elastic angular distributions such as sharp minima would tend to be averaged out. Individual differences in nuclear properties, such as the variation of V from one nuclide to another, would be missed. For example, at a closed shell of the independent-particle model, the nuclear potential might be noticeably different than at a partially filled shell. Sizable impurities in the isotopic composition of a target element could thus contribute unpredictable effects in a measurement of an elastic scattering cross section.

It was hoped that the present experiment could investigate these effects. To this end, isotopically pure targets were used whose nuclei involved numbers of protons and neutrons near shell number 28. Our proton detector could distinguish elastic from nonelastic scattering in the angular range 0° to 110° for most target elements used. The angular resolution of the detection system was good enough to define accurately the features of the diffraction scattering.

It should finally be noted that most of the optical-model analyses of intermediate-energy proton scattering (5 to 40 Mev) have omitted consideration of potential spin-orbit effects and nonspherical well shapes. Polarization experiments are required to measure the effects of the former unambiguously. However, sufficiently accurate ordinary proton scattering data could possibly show effects of the latter, especially near the region of magic number nuclei.

II. EXPERIMENTAL APPARATUS

A beam of protons magnetically deflected from the exit of the second section of the Minnesota linear accelerator possesses the following approximate characteristics: angular deviation, ± 1.5 milliradians; maximum time average current, 4×10^{-8} ampere with a repetition rate of 30 pulses per second; beam pulse length 150 microseconds; and beam energy 39.85 ± 0.20 Mev. This beam passed successively through a quadrupole lens system, a 0.001-in. Duralumin foil (separating the scattering chamber from the accelerator vacuum system) defining and antiscattering apertures, a scattering

[8] R. D. Woods and D. S. Saxon, Phys. Rev. **95**, 577 (1954).

chamber,[9] a 0.003-in thick Mylar window to the scattering chamber, 3 in. to 18 in. of air, and another Duralumin foil which served as the entrance to a beam collecting Faraday cup.

The path of detected protons scattered from a target led through the Mylar window of the scattering chamber into the atmosphere, where a detector telescope was placed at some known distance from the target. Protons passed through this telescope into a NaI(Tl) scintillation crystal where they were detected and stopped.

The experimental scattering assembly is shown in Figs. 1 and 2. It consists of an 8-ft diameter stand[9] upon which are mounted two arms each independently free to rotate through 360°. The 12-in. diameter scattering chamber[9] was placed at the center of this stand so that targets could be isolated from atmospheric scattering elements.

Five nuclides were used as targets in these measurements: Fe^{54}, Fe^{56}, Ni^{58}, Ni^{60}, and Cu^{65}.[10] Their isotopic composition was determined by the Oak Ridge laboratory at their time of fabrication. Except for the iron target, which was 95% Fe^{54}, the targets were monoisotopic to greater than 98%. They were approximately 50 mg/cm² thick.

The general detection scheme is shown in Fig. 2. The telescope arrangement was used to shield the NaI(Tl) crystal from charged particles emanating elsewhere than in the target. Antiscattering baffles were placed inside the telescope to prevent particles not within the solid angle of the detector from entering the NaI(Tl) crystal. Light pulses formed in the crystal were channelled through a Lucite light pipe into a Dumont 6292 photomultiplier tube. The resulting pulse was amplified in a conventional fashion and registered on a pulse-height analyzer.

Various detector solid angles were employed in the course of the measurements.

For most target elements it was found that to separate clearly adjacent peaks displayed on a pulse-height spectrum, one corresponding to protons elastically scattered and the other to protons nonelastically scattered from the first excited state of the target nucleus, an energy resolution better than 1.5% was required (full width at half maximum). To obtain such energy resolution it was found necessary to insert a cylindrical Lucite light pipe between the crystal and the photomultiplier tube. By thus placing the photocathode at an extended distance from the crystal and diffusing the light transmitted to it, the light intensity distribution over the photocathode of the photomultiplier tube for each elastic proton scintillation emitted by the crystal was equalized. Enough light was available from the scintillations of a 40-Mev proton so that attenuation of the light intensity in the light pipe was of small concern.

To attain the required energy resolution it was necessary also to prevent the pileup of pulses in the crystal and electronics. This was accomplished by shielding the crystal from background radiation and by counting slowly when the number of nonelastic pulses was relatively large compared to elastic pulses.

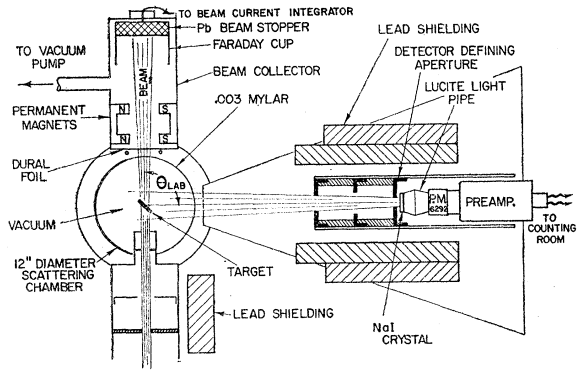

FIG. 2. A detailed view (not to scale) of the proton-scattering system.

III. EXPERIMENTAL DATA

A. Procedures

Discussed here are effects which could have influenced the accuracy of the measurements.

The first concerns the anomalous scattering of protons into the detector: (1) from the window of the scattering chamber, or (2) from the target holder. Both (1) and (2) were accounted for through background measurements when the proton beam was passed through empty target holders. For angles greater than 20°, this background was negligible. Background due to slit scattering associated with the detector telescope would not have been detected by removing the target from the beam. It was eliminated as a possible source of error by varying the detector telescope dimensions in an otherwise fixed geometry. No differences in scattering yields were found when this was done.

A second set of effects which tends to obscure the energy separation of elastically and nonelastically scattered protons, concerns poor energy resolution and possible nonlinearities in the detection system. To investigate the linearity and energy resolution of the equipment, protons were scattered from CH_2 foils. The equipment was calibrated by comparing positions on the pulse-height analyzer spectrum of elastically scattered protons from both C^{12} and H^1, and nonelastically scattered protons from the 4.4-Mev excited state of C^{12}.

B. The Data

The energy of the incident protons for all cross section measurements was 39.8±0.2 Mev.

The range of the angular distributions, from 7.5° to 110°, was the same for all elements investigated. For

[9] M. K. Brussel and J. H. Williams, Phys. Rev. **106**, 286 (1957).
[10] We are indebted to the Oak Ridge National Laboratory for fabricating these targets (electroplating process).

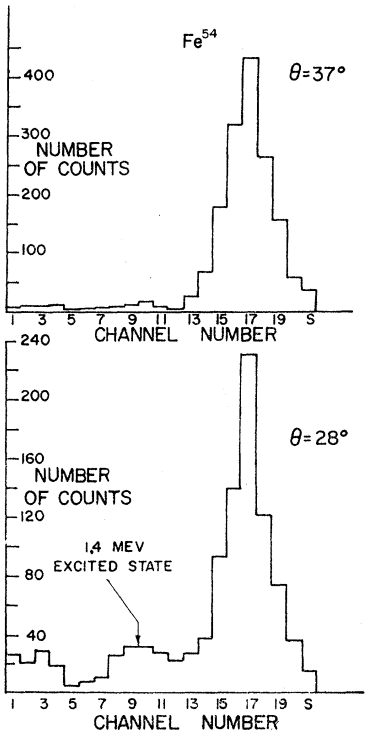

FIG. 3. Pulse-height distributions of protons scattered from Fe^{54}. The top figure shows a distribution taken at a maximum of the angular distribution; at bottom is one taken at the first minimum of the angular distribution. The energy scale is given by the distance between the elastic (39.8 Mev) peak and the nonelastic peak 1.4 Mev distant in energy.

this range of angles, all protons entering the detector passed through any layer of the target only once ("in transmission"). This made it possible to maintain the 1.5% energy resolution.

Due to background effects and the finite energy resolution of the detection equipment, some ambiguity always occurred in determining the number of counts in the pulse-height spectrum that represented truly elastically scattered protons. The determination of this number of counts was judged from symmetry considerations of both elastic and first nonelastic peaks in the pulse-height spectrum. It was assumed that the nonelastic spectrum would have the same width and shape as the elastic spectrum. With this assumption, together with the assumption that the high-energy side of the elastic peak represented the true shape of the elastic spectrum, one could estimate the overlap of elastic and nonelastic peaks. In addition, plots of the nonelastic proton scattering from the first excited state of the target nucleus were constructed. Assuming that the nonelastic cross sections varied smoothly with angle, a nonelastic cross section appearing grossly different from its neighboring (in angle) cross sections was adjusted to lie closer to the smooth curve determined by them, and the assignment of counts in the pulse-height spectrum was correspondingly changed in calculating the associated elastic cross section. In most instances, the nonelastic cross sections were small fractions of the elastic cross section. Therefore, any corrections in the nonelastic cross-section calculations affected the elastic cross-section determinations to a correspondingly lesser degree. Near minima in the angular distributions of the elastically scattered proton data, however, this was not generally true, especially when the energies of the elastic and nonelastic protons lay close together. Figure 3 displays some typical pulse-height spectra.

With the exception of only a few cases, the number of counts recorded under the elastic scattering peak of a pulse-height spectrum was such that the standard deviation was less than 3.3%. In most instances it was closer to 2.5%.

As may be noticed from a displayed pulse height spectrum of the elastic scattering, counts appeared in the surplus channel of the pulse-height analyzer. (On all pulse-height distributions, the absolute energy scale can be determined by noting the difference in scale position between the elastic and nonelastic peaks of the spectrum for the element concerned.) These represented pulses of higher energy release in the crystal than elastically scattered protons. Such pulses were considered as elastically scattered protons.

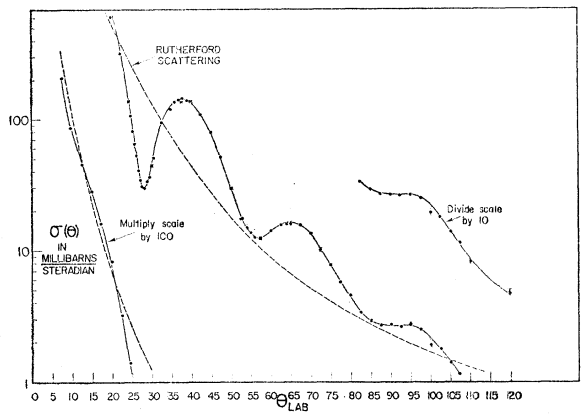

FIG. 4. The angular distribution of 39.8-Mev proton elastic scattering from Fe^{54}. The illustrated typical errors include statistical and nonelastic scattering errors only. The dashed curve is one calculated for point-charge Rutherford scattering.

As mentioned, background was negligible at angles above 20°. Below 20°, background corrections were applied to the data to account for protons scattered from the beam-collimating slits or from the Mylar exit window of the scattering chamber.

Another correction which was applied to all the data concerned the effects of nuclear interactions made by protons entering the NaI detector crystal. Such interactions would tend to decrease the measured elastic scattering cross sections. Johnston and Swenson[11] have

[11] L. H. Johnston and D. A. Swenson, Phys. Rev. **111**, 212 (1958).

investigated this effect carefully and have come to the conclusion that (for 40-Mev protons) a 1.9% correction should be applied to the data to account for it. This correction has been applied.

Cross sections tabulated in this paper are in the laboratory system of coordinates. The difference between these and center-of-mass cross sections amounts to about 3% below 30°, 2% at 45°, and 1% at 60°, with no correction at 90°.

All formulas used in these calculations are nonrelatavistic. The errors involved due to use of nonrelativistic formulas amounts to less than 0.3%.

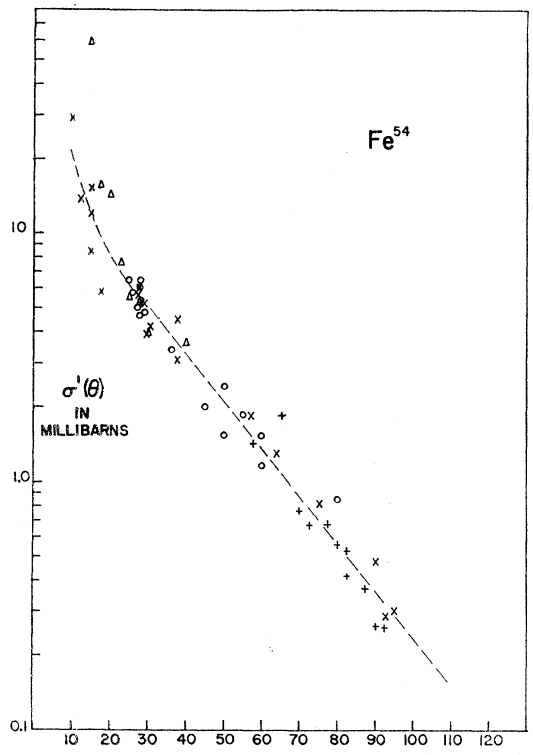

FIG. 5. Angular distribution of protons nonelastically scattered from the 1.4-Mev excited state of Fe^{54}. The dashed curve was drawn by eye through the experimental points to provide average values for the nonelastic scattering corrections to elastic scattering data. The abscissa is the scattering angle, θ, in degrees. The different symbols represent different runs.

In the following sections, the elements with which cross-section angular distributions were obtained are discussed individually.

Fe^{54}

Data are displayed in Fig. 4.

The first excited state of Fe^{54} occurs[12] at approximately 1.4 Mev and could in general be distinguished in the raw data. Examples of pulse-height spectra obtained are given in Fig. 3. The energy resolution (full width at half maximum) of the detection system was approximately 1.75%; at times, as good as 1.25%.

[12] Winham, Gossett, Phillips, and Schiffer, Phys. Rev. **103**, 1321 (1956).

TABLE I. Ratio of elastic cross sections to 1.4-Mev nonelastic cross sections.

Angle (deg)	Elastic/nonelastic
7.5	55
15.0	33
27.5	6
35.0	33
55.0	7
65.0	14
90.0	6
110.0	5

Nonelastic differential cross sections of the scattering from the 1.4-Mev excited state calculated in the course of analyzing the elastic data are given in Fig. 5. Over the range of angles at which data were obtained, the elastic scattering cross sections were from 5 to 55 times the inelastic cross sections. Table I shows the approximate ratios at various angles.

Fe^{56}

The Fe^{56} angular distribution is given in Fig. 6. Some pulse-height distributions are given in Fig. 7. The elastic scattering cross sections were derived principally by "symmetrizing" the elastic peak in the pulse-height spectra.

Figure 8 gives the ratio of the elastic to nonelastic cross sections. It should be noted that this graph is accurate only to about ±40%. This was to be expected for an element like Fe^{56} where the nonelastically scattered protons arose from an excited state at 0.845 Mev, relatively close to the ground state. The resolution available at the time of these measurements was not sufficient to separate this scattering from elastic scattering.

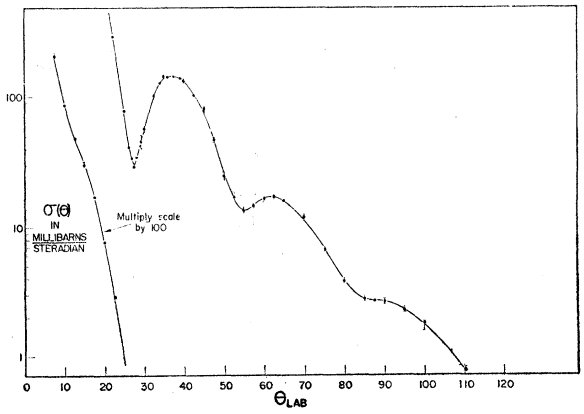

FIG. 6. The angular distribution of 39.8-Mev proton elastic scattering from Fe^{56}. The illustrated typical errors include statistical and nonelastic scattering errors only.

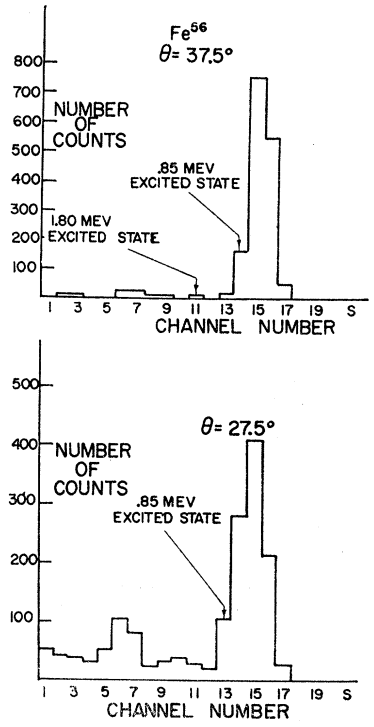

FIG. 7. Pulse-height spectra from Fe^{56} at a maximum (top) and minimum (bottom) of the angular distribution. The energy scale is given by the distance between the elastic scattering peak at 39.8 Mev and the nonelastic scattering peaks 0.85 Mev and 1.80 Mev lower in energy.

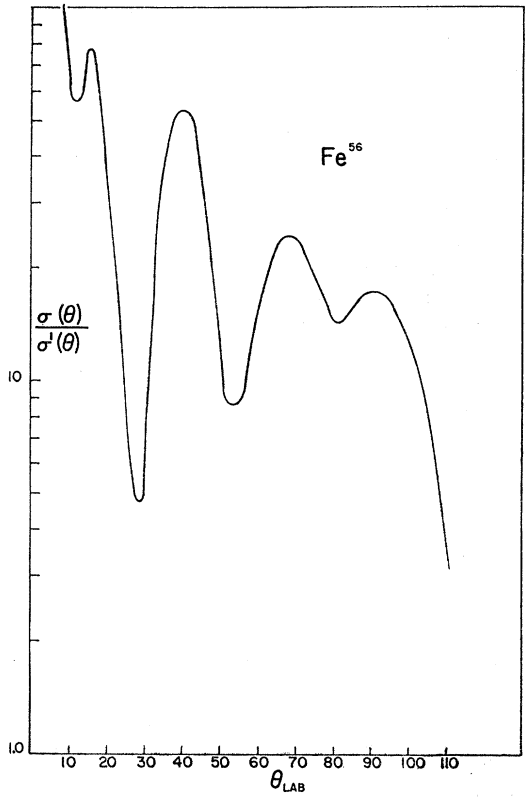

FIG. 8. The Fe^{56} ratio of elastic to nonelastic scattering, $\sigma(\theta)/\sigma'(\theta)$, as a function of scattering angle, θ_{lab}. The nonelastic scattering is due to the 0.845-Mev excited state of Fe^{56}. The curve was drawn through experimental points accurate to about $\pm 40\%$.

Ni^{58}

The angular distribution for Ni^{58} is given in Fig. 9. The first excited state of Ni^{58} lies at 1.45 Mev. It appeared that the ratio of elastic to nonelastic scattering (Fig. 10) from this state was greater than for Fe^{56}, but was about the same as for Fe^{54}.

Ni^{60}

The Ni^{60} angular distribution is shown in Fig. 11. The first excited state in Ni^{60} appears at 1.33 Mev and could generally be resolved. The ratio of differential elastic to nonelastic scattering appeared quite similar to the Ni^{58} case.

Cu^{65}

Cu^{65} has a first excited state at 0.815 Mev, and another excited state at 1.15 Mev,[13] scattering from neither level being unambiguously distinguishable from elastic scattering. Figure 12 illustrates the angular distribution.

The energy resolution of the detection system for the Cu^{65} data was approximately 1.8%. The amount of nonelastic scattering relative to elastic scattering was, Fe^{56} excepted, about the same as for the other elements.

[13] G. M. Temmer and N. P. Heydenburg, Phys. Rev. 104, 967 (1956).

C. Errors

The errors for the present measurements were found to be strongly dependent upon the scattering angle at which the measurement was taken and upon the particular isotope used as a target. Sources of errors are discussed below.

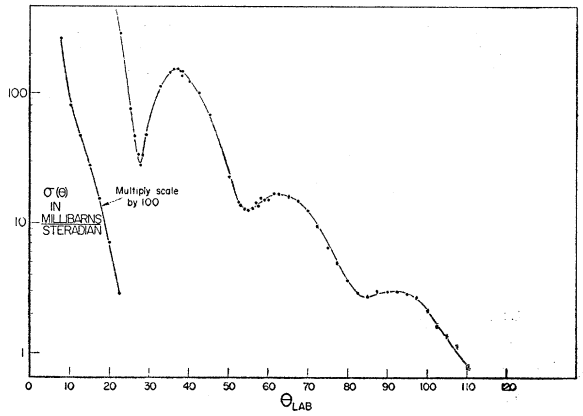

FIG. 9. The angular distribution of 39.8-Mev proton elastic scattering from Ni^{58}. The illustrated typical errors include statistical and nonelastic scattering errors only.

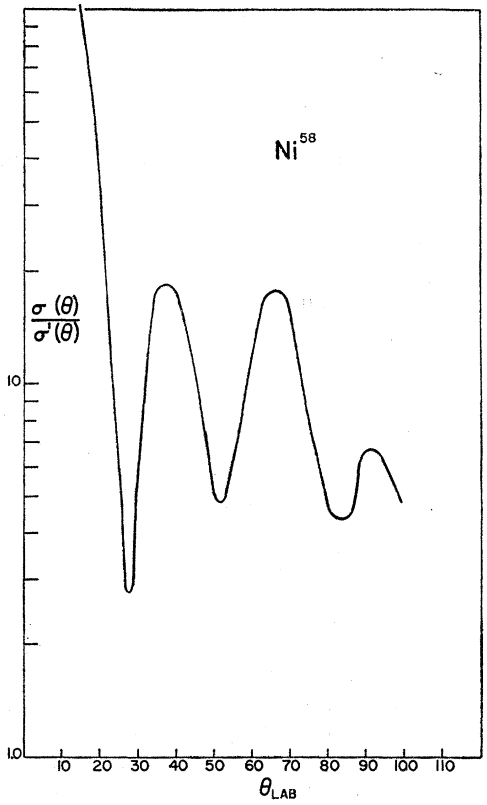

FIG. 10. The ratio of elastic to nonelastic scattering from Ni^{58} as a function of the scattering angle. The nonelastic scattering is due to the 1.3-Mev excited state in Ni^{58}.

The error due to geometrical factors includes not only the measurement of detector dimensions, but the accuracies to which scattering angles and angles of the target to the beam line were known. Thus, given an error of $\pm 0.15°$ for the angular position of the detector, a cross-section error contribution from zero (at maxima of the angular distributions) to about 7.5% (where the cross sections were changing most rapidly with angle) would be made. Similarly, the angle of the target could be determined to only $\pm 1.5°$. This corresponded to a possible error of as much as 3% at 45° orientation to the beam.

Beam current collection errors also varied according to the detection angle, for where cross sections were large the beam was made correspondingly small (to prevent pileup) and the effect of drifts in the beam-current integration circuit would be magnified. Except at the smallest scattering angles, this drift contributed cross-section errors estimated to be 1%.

Multiple scattering introduced significant error only at the first minimum in the angular distribution where the change in the slope of the angular distribution was large. Here, more particles would be scattered into the detector than out of it. This effect could have been as high as 10%.

Nonelastic scattering contributions to the measured elastic cross sections also were a function of scattering angle. An over-all average estimate of such errors, however, is about 3%. The statistical accuracy of most points at which measurements were taken was also 3%.

Target thicknesses for Fe^{54}, Fe^{56}, and Ni^{58}, were determined to 1%. Ni^{60} and Cu^{65} targets, due to their nonuniform thickness, were determined to 4% and 3%, respectively. These targets were less massive at their centers where the proton beam passed than at their periphery, so that an average thickness (in grams/cm^2) determined by weighing the targets and measuring their surface areas had to be corrected to represent that thickness which was presented to the beam. The increased errors reflect these corrections.

To summarize: The probable error for the experimental unaveraged absolute cross sections lies from $\pm 6\%$ to $\pm 10\%$ for Fe^{54}, Fe^{56}, Ni^{58}, and from $\pm 7\%$ to $\pm 11\%$ for Ni^{60} and Cu^{65}. Averaged data would cancel out much of the detector "angular" and "beam energy shift" errors because of their expected random nature.

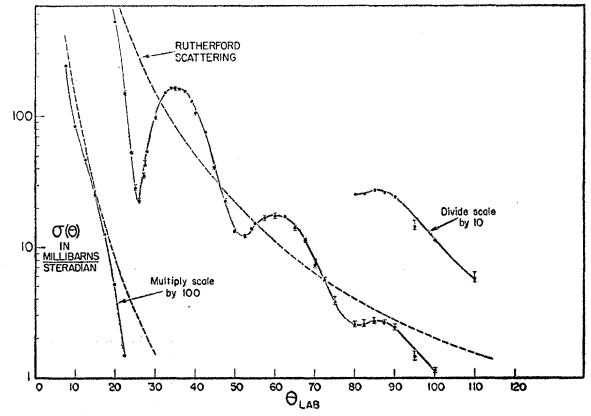

FIG. 11. The angular distribution of 39.8-Mev proton elastic scattering from Ni^{60}. The illustrated typical errors include statistical and nonelastic scattering errors only. The dashed curve is one calculated for point-charge Rutherford scattering.

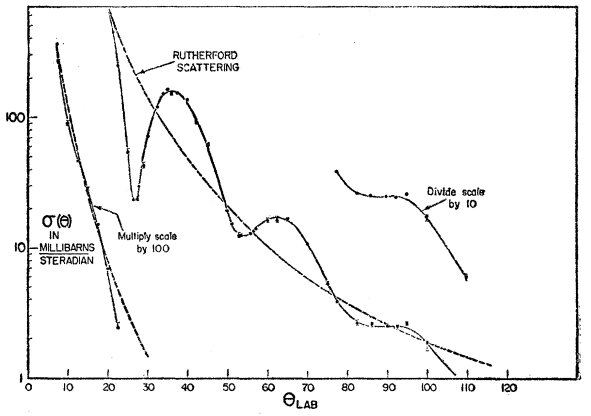

FIG. 12. The angular distribution of 39.8-Mev proton elastic scattering from Cu^{65}. The illustrated typical errors include statistical and nonelastic scattering errors only. The dashed curve is one calculated for point-charge Rutherford scattering.

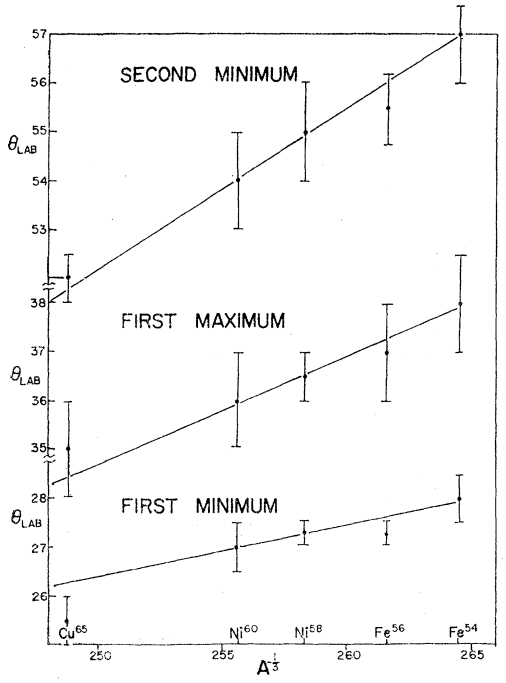

FIG. 13. The angle at which specific features listed above appear in the elastic scattering angular distributions is plotted as a function of the inverse cube root of the atomic number, A.

Since the data presented have been averaged and represent the results of multiple data-accumulating periods, it is believed that they are, on the whole, accurate to 6%. Relative cross-section data would be somewhat more accurate, as would cross-section data at maxima in the diffraction pattern. Conversely, at minima, cross sections would be less accurate.

D. Discussion of Results

The present measurements were undertaken to exhibit any finer structure in the cross-section behavior than might be expected from simple diffraction theory arguments. Though it has been found, subsequent to completion of the present work, that yet more accurate measurements are needed to identify such effects positively and to measure their magnitudes, scattering anomalies do appear in the present work that suggest fine-structure effects, such effects probably being somehow linked with shell effects in the target nuclei.

In Fig. 13, angles at which specific features occur in the differential cross sections, are plotted as a function of the inverse cube root of the atomic number. Such a plot over a broad range of A has shown[3] a constant relation between A and θ_i (the angle at which feature i occurred). This was interpreted as an indication of the essential optical character of the scattering. One would have expected such a relationship for $\theta_i \lesssim 60°$.

The angular errors shown in Fig. 13 indicate mainly the broadness of the angular features in the data. Though these errors would allow straight lines to be drawn through all five points on this graph, it was noticed that if one considered the "magic number" nuclei Fe^{54}, Ni^{58}, and Ni^{60}, then for all three features plotted, straight lines could be drawn through the precise angles assigned to the features. The other elements, Fe^{56} and Cu^{65}, do not in general lie on this line. It might be expected, from the way in which the independent-particle model potential well depth and radius parameter are known to vary[14] (as reflected by nuclear binding energies and isotope shifts, for example) as one passed through a closed-shell nucleon configuration, that anomalous behavior in scattering characteristics would be observed if scattering features between them were compared. Thus, if one postulated independent-particle orbits for the scattering particle, the anomalously smaller nuclear core that magic nuclei may possess would cause a relatively more dilated scattering pattern. The present data suggest such arguments though the Cu^{65} behavior seems inconclusive.

IV. CONCLUSIONS

In the present measurements it is difficult to discern qualitative differences in the shapes of the various angular distributions. Nevertheless, some features of the cross sections do occur which suggest that the analytical shapes of the curves differ. For example, whereas Fe^{54} variations are generally stronger than those of Fe^{56}, this does not appear to be true at the first maximum.

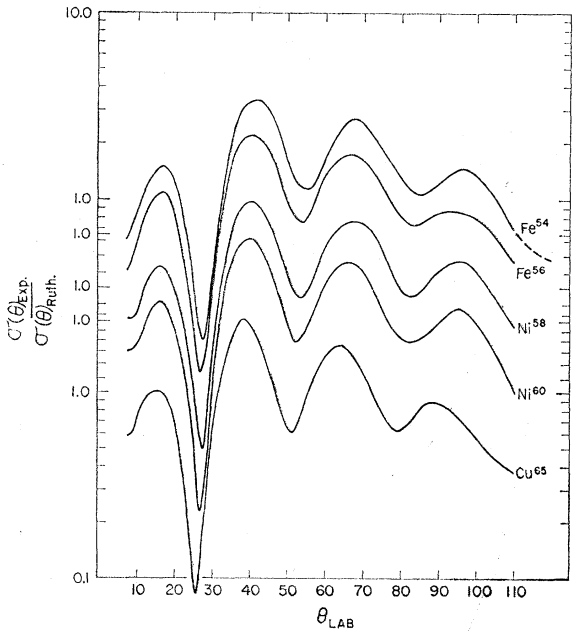

FIG. 14. The ratio of the experimentally determined elastic scattering cross sections to the Rutherford cross sections is plotted as a function of the scattering angle for all the nuclides measured in this work. The ordinate scales are displaced vertically as indicated.

[14] M. G. Mayer and J. H. D. Jensen, *Elementary Theory of Nuclear Shell Structure* (John Wiley & Sons, Inc., New York, 1955).

Similarly, though Ni^{58} and Ni^{60} are comparable feature for feature below 75°, thereafter they appear to diverge (σ for $Ni^{58} < \sigma$ for Ni^{60}). It should be cautioned, however, that it is difficult to compare these elements without some quantitative analysis that would clearly describe in what sense these elements tended to be equivalent. For example, one would expect a Rutherford normalization to be a valid physical representation only at forward angles.

The over-all changes expected on the basis of simple arguments are evident from the data; i.e., the way in which the ratio σ(experimental)/σ(Rutherford) varies with A (see Fig. 14), and the way θ_i varies with A.

The practical results of the experiments are, then, that the general features are not greatly changed by using naturally occurring isotopes as targets. Only if one is seeking yet finer effects than the present measurements allow, could this be an important factor. The optical model analyses so far attempted have been directed towards finding average values of nuclear parameters and have not attempted to predict rapid changes of these parameters between neighboring nuclei. The present measurements justify this approach by indicating that no gross effects are seen. The present data do suggest however, that small differences in the shapes of the angular distributions do exist and should be accounted for.

ACKNOWLEDGMENTS

It is with pleasure that we acknowledge illuminating discussions with Professor Norton Hintz throughout the course of these measurements. We extend our thanks also to Professor Lawrence Johnston and Dr. Donald Swenson whose work on NaI nuclear interactions we have utilized, and to the whole operating staff of the Minnesota Linac.

PHYSICAL REVIEW VOLUME 114, NUMBER 2 APRIL 15, 1959

Study of (d,α) Reactions on Some Light Nuclei*

G. E. FISCHER AND V. K. FISCHER
Columbia University, New York, New York, and Brookhaven National Laboratory, Upton, New York

(Received November 26, 1958)

The angular distributions of the charged particles from the $N^{14}(d,d)N^{14}$, $N^{14}(d,\alpha_0)C^{12}$, $N^{14}(d,\alpha_1)C^{12*}$, and $N^{15}(d,\alpha_0)C^{13}$ reactions have been studied with a deuteron bombarding energy of 21 Mev. The charged-particle groups are identified and their energy is measured by a dE/dX *vs* E counter telescope. The $N(d,\alpha)C$ angular distributions and the $O^{16}(d,\alpha)N^{14}$ angular distribution measured by Freemantle *et al.* have been compared with theoretical curves calculated from a simplified direct-interaction model. The relative magnitudes of the experimentally determined cross sections have also been compared with theory. The results indicate that the $O^{16}(d,\alpha_0)$ reaction can be described by the compound-nucleus extreme, while the $N^{14}(d,\alpha_1)$ process appears to favor description by a direct-interaction model. The remaining (d,α) reactions are intermediate cases.

INTRODUCTION

MANY investigators have pointed out that nuclear reactions which involve incident particles with energies from 10 to 50 Mev and in which the final nucleus is left in a low-lying state, proceed predominantly by a direct process in which the incoming particle interacts with only one or a few nucleons of the initial nucleus. However, the compound-nucleus picture remains an adequate description of the majority of nuclear reactions. Theoretical cross sections have been derived for both treatments[1,2] and for convenience these will be used in the discussion of experimental results. Actually, it must be remembered that no sharp distinction exists, but there is instead a theoretically difficult intermediate region. Lane and Thomas[3] have discussed how the R-matrix formalism can be used for the whole range of reaction types, but their theory has not been worked out in detail for direct reactions.

In the case of reactions in which complex particles are involved, the theoretical direct-interaction treatment is necessarily based on simplified models. Yet in the (α,p) case, surprisingly good agreement with experi-

* This work partially supported by the U. S. Atomic Energy Commission.

[1] A partial list of theoretical papers on direct reactions: S. T. Butler, Proc. Roy. Soc. (London) **A208**, 559 (1951); R. Huby and H. C. Newns, Phil. Mag. **42**, 1443 (1951); Austern, Butler, and McManus, Phys. Rev. **92**, 350 (1953); W. Tobocman and M. H. Kalos, Phys. Rev. **97**, 132 (1955); L. Madansky and G. E. Owen, Phys. Rev. **99**, 1608 (1955); D. M. Brink, Proc. Phys. Soc. (London) **A68**, 994 (1955); Hayakawa, Kawai, and Kikuchi, Progr. Theoret. Phys. Japan **13**, 415 (1955); **14**, 1 (1955); S. Yoshida, Proc. Phys. Soc. (London) **A69**, 668 (1956); J. R. Lamarsh and H. Feshbach, Phys. Rev. **104**, 1633 (1956); L. R. B. Elton and L. C. Gomes, Phys. Rev. **105**, 1027 (1957); C. A. Levinson and M. K. Banerjee, Ann. Phys. N. Y. **2**, 471 (1957); S. T. Butler, Phys. Rev. **106**, 272 (1957); N. Austern and S. T. Butler, Phys. Rev. **109**, 1402 (1958).

[2] For compound-nucleus theory see J. M. Blatt and V. F. Weisskopf, *Theoretical Nuclear Physics* (John Wiley & Sons, Inc., New York, 1952), or any similar text.

[3] A. M. Lane and R. G. Thomas, Revs. Modern Phys. **30**, 257 (1958).